

pubs.acs.org/JACS Communication

Synergetic Bottom-Up Synthesis of Graphene Nanoribbons by Matrix-Assisted Direct Transfer

Ryan D. McCurdy,^{\$} Peter H. Jacobse,^{\$} Ilya Piskun, Gregory C. Veber, Daniel J. Rizzo, Rafal Zuzak, Zafer Mutlu, Jeffrey Bokor, Michael F. Crommie, and Felix R. Fischer*



Cite This: J. Am. Chem. Soc. 2021, 143, 4174-4178



ACCESS

III Metrics & More





ABSTRACT: The scope of graphene nanoribbon (GNR) structures accessible through bottom-up approaches is defined by the intrinsic limitations of either all-on-surface or all-solution-based synthesis. Here, we report a hybrid bottom-up synthesis of GNRs based on a Matrix-Assisted Direct (MAD) transfer technique that successfully leverages technical advantages inherent to both solution-based and on-surface synthesis while sidestepping their drawbacks. Critical structural parameters tightly controlled in solution-based polymerization reactions can seamlessly be translated into the structure of the corresponding GNRs. The transformative potential of the synergetic bottom-up approaches facilitated by the MAD transfer techniques is highlighted by the synthesis of chevron-type GNRs (cGNRs) featuring narrow length distributions and a nitrogen core-doped armchair GNR (N_4 -7-ANGR) that remains inaccessible using either a solution-based or an on-surface bottom-up approach alone.

₹ he bottom-up synthesis of graphene nanoribbons (GNRs), quasi-1D strips of graphene that can host precisely tunable band gaps and topological engineered states, has largely been restricted to two complementary but mutually incompatible approaches. 1-7 The first is an on-surface catalyzed radical step-growth mechanism well-suited for the detailed characterization of GNRs using advanced scanning probe microscopy (SPM) imaging and spectroscopy. The second is a more conventional solution-based approach that takes advantage of the superior control over critical performance parameters provided by modern step-growth and living polymerization techniques.^{8,9} While the first technique has been a workhorse for the exploration of electronic properties emerging from lateral quantum confinement in graphene, the control over critical structural parameters, e.g., GNR length, monomer sequence, number and position of interface states, and functional end-groups has been limited by the shortcomings of surface-catalyzed radical step-growth polymerization. 10 In contrast, solution-based approaches can overcome many of the structural limitations encountered in the onsurface growth. Modern synthetic protocols give access to sequence controlled (co)polymer precursors to functional GNRs. Both the length and functional end-groups can be precisely controlled using living polymerization techniques.¹¹ For either technique, the scope of the synthetically accessible GNR structures is largely dictated by unique sets of requirements imposed by either the underlying surface-growth or solution-based polymerization mechanisms and are often exclusive to either technique. 12,13 Leading efforts to integrate bulk solution-synthesized GNRs with advanced surface-based characterization tools have relied on a direct contact transfer (DCT) sample preparation technique.¹⁴ While this approach has successfully been used to characterize solution-synthesized GNRs using SPM, the sample preparation suffers from the common trend of GNRs to aggregate into amorphous bundles

through $\pi-\pi$ stacking interactions. ^{14,15} Furthermore, DCT of fully cyclized solution-synthesized GNRs fails to take advantage of a wealth of chemical transformations and structures exclusively accessible through on-surface growth techniques. ^{5,16,17}

We herein report a hybrid bottom-up approach that successfully combines three key elements of advanced GNR synthesis: (i) the exquisite structural control provided by solution-based polymerization techniques gives access to sequence-controlled (co)polymer GNR precursors featuring narrow and well-defined length distributions, (ii) matrix-assisted direct (MAD) transfer (Figure 1) of these GNR precursors onto solid substrates, e.g., Au(111), enables surface catalyzed chemical transformations widely used in the onsurface synthesis of GNRs, (iii) preparation of spatially isolated GNRs on scanning tunneling microscopy (STM) compatible substrates gives access to advanced bond-resolved imaging and spectroscopic characterization techniques previously reserved for surface grown GNRs.

We initially studied the thermally induced surface catalyzed cyclodehydrogenation of *poly-1* (Scheme 1), a precursor to chevron-type GNRs (cGNRs), deposited on Au(111) surfaces using our MAD transfer technique. Size exclusion chromatography (SEC) analysis of samples of *poly-1* prepared through $Ni(cod)_2$ catalyzed *Yamamoto* step-growth polymerization ¹⁸ of 6,11-dibromo-1,2,3,4-tetraphenyltriphenylene exhibit broad molecular weight distributions (D = 1.3, SI Figures S1 and

Received: February 3, 2021 Published: March 12, 2021





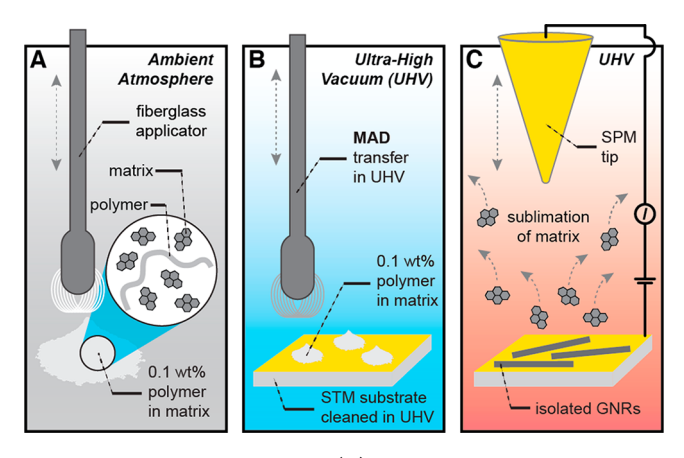


Figure 1. MAD transfer process: (A) Loading of fiberglass applicator with polymer sample dispersed in an inert matrix under ambient conditions; (B) MAD transfer of polymer dispersion onto STM substrate in ultrahigh vacuum (UHV); (C) annealing induces traceless sublimation of bulk matrix followed by cyclodehydrogenation leaving spatially isolated GNRs behind.

Scheme 1. Bottom-Up Synthesis of cGNRs using a MAD Transfer of *poly-*1 Followed by Thermal Cyclodehydrogenation

S2) and M that ranges between 2–12 kg mol⁻¹. Preparative SEC of a crude sample of poly-1 soluble in CHCl₃ yielded a low M_n fraction poly-1a (M = 2-7 kg mol⁻¹) and a high M_n fraction poly-1b (M = 7-12 kg mol⁻¹). Matrix-assisted laser desorption ionization time-of-flight mass spectrometry (MALDI-TOF MS) of poly-1a (Figure 2A) shows a family of peaks separated by integer repeat units of the monomer mass ($\Delta m/z = 530$ u) ranging from the 5mer to the 13mer, m/z = 2661 u to m/z = 6905 u, respectively. MALDI of the high

 $M_{\rm n}$ fraction poly-1b (Figure 2B) reveals an analogous series of mass signals ($\Delta m/z = 530$ u) ranging from the 15mer to the 22mer (m/z = 7968 u to m/z = 11681 u), albeit at significantly lower intensities. End-group analysis suggests that the polymers are terminated by hydrogen atoms on either end of the chain.

With two unique fractions of poly-1 in hand we set out to prepare samples for MAD transfer onto Au(111) substrates. Selection of a suitable matrix requires consideration of both chemical and materials properties. The matrix itself must be chemically inert across a wide range of temperatures to avoid undesired reactions with the polymer sample or uncontrolled thermal decomposition during processing. A low melting point, $T_{\rm m}$, ensures that the polymer can readily be dissolved in a melt of the matrix under ambient conditions. Dispersion and dilution of the polymer sample is most effective if the noncovalent interactions between the matrix and the polymer sample are stronger than the attractive interactions between molecules of the sample themselves. Traceless removal of the matrix following deposition can only be achieved if the matrix exhibits a low enthalpy of sublimation, $\Delta H_{\text{sub}}^{\circ}$, and undergoes a solid/gas phase transition in UHV. While a wide variety of polycyclic aromatic hydrocarbons meet the criteria listed above, we herein relied on pyrene ($T_{\rm m}$ = 151.1 \pm 0.5 °C, $\Delta H_{\rm sub}^{\circ} = 23.9 \pm 0.3$ kcal mol⁻¹) as a universally accessible traceless matrix.

Dispersions of poly-1a and poly-1b (0.1 wt %) in a melt of pyrene were prepared and rapidly solidified at -78 °C before being ground into a fine powder and deposited in UHV onto a Au(111) surface using a fiberglass stamp (Figure 1). Annealing of the molecule-decorated surface at 300 °C for 10 min in UHV induces sublimation of the bulk matrix (~99 wt % pyrene). STM images on Au(111) reveal a submonolayer coverage of the surface with islands of parallel aligned chains of poly-1 separated by a random network of residual pyrene molecules (Figure 2C). The characteristic adsorption geometry and structural features of poly-1 synthesized in solution and deposited by MAD transfer on a Au(111) surface are indistinguishable (0.28 \pm 0.03 nm, 1.5 \pm 0.1 nm, 1.5 \pm 0.1 nm, height, width, and length of the polymer repeat unit) from an original sample prepared via a surface catalyzed radical step growth polymerization of 6,11-dibromo-1,2,3,4-tetraphenyltriphenylene on Au(111).3 Further annealing of the sample at 420 °C for 10 min induces a thermal cyclodehydrogenation that transforms the polymer precursor poly-1 into the fully conjugated backbone of cGNRs (Figure 2D,G). STM topographic images reveal the characteristic structural features of cGNRs (0.18 \pm 0.03 nm, 2.5 \pm 0.2 nm, 1.5 \pm 0.1 nm, height, width, and length of the GNR repeat unit) separated by isolated matrix molecules (Figure 2D).3,22 Extending the annealing step from 10 to 30 min leads to the complete desorption of the remaining submonolayer of pyrene leaving only cGNRs behind (Figure 2H). Direct comparison with a sample of poly-1 deposited on Au(111) using a matrix-free DCT technique serves to highlight the critical role of the pyrene matrix in our MAD transfer process. STM topographic images reveal that, in the absence of a matrix, thermal annealing of poly-1 leads exclusively to irregular carbon networks rather than discrete cGNRs (SI Figure S3).

To demonstrate the potential of our MAD transfer process we recorded large area topographic STM images and performed statistical length analysis of cGNRs grown from samples of poly-1a ($M = 2-7 \text{ kg mol}^{-1}$, 5–13 monomers

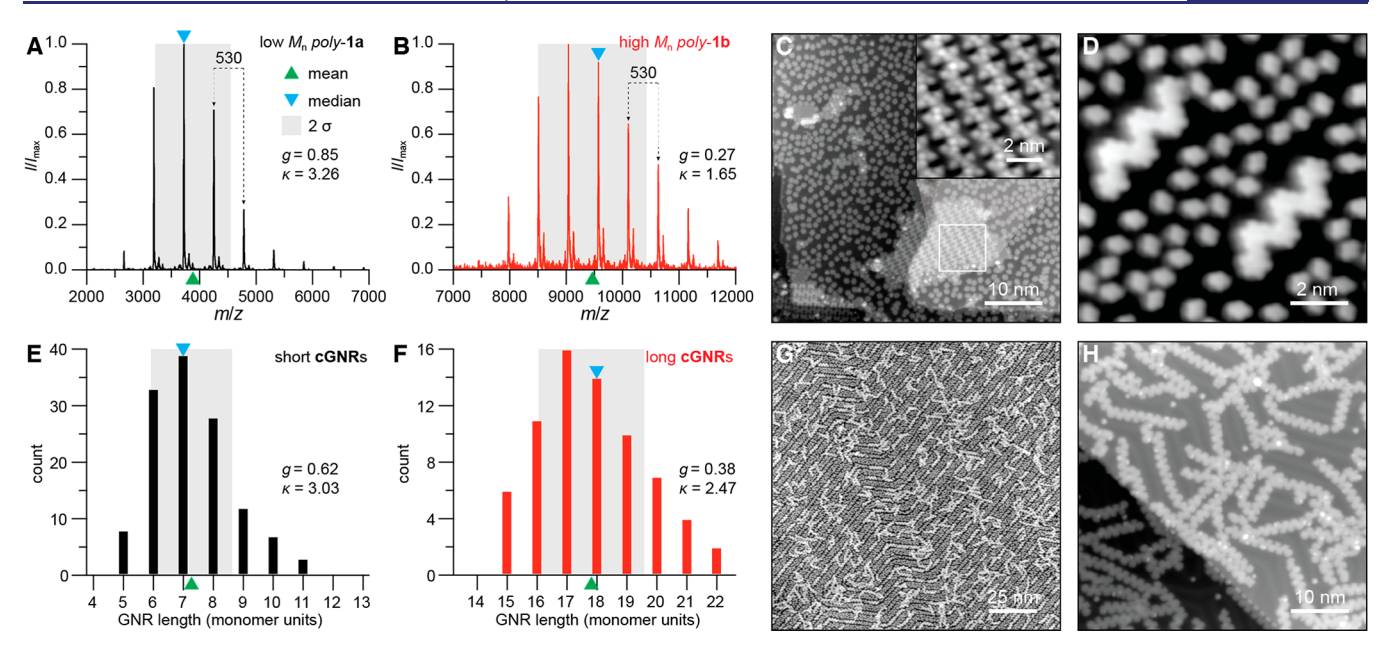


Figure 2. MALDI-TOF MS of (A) poly-1a and (B) poly-1b. (C) STM topographic image ($V_s = -2.0 \text{ V}$, $I_t = 50 \text{ pA}$) of poly-1b deposited on a Au(111) surface using MAD transfer followed by sublimation of the bulk pyrene matrix at 300 °C for 10 min. The inset shows a self-assembled island of uncyclized poly-1b ($V_s = -2.0 \text{ V}$, $I_t = 100 \text{ pA}$). (D) STM topographic image of short cGNRs resulting from annealing of a MAD-transferred sample of poly-1a to 420 °C for 10 min ($V_s = 0.3 \text{ V}$, $I_t = 200 \text{ pA}$). Histogram of cGNR length resulting from (E) poly-1a ($N_s = 1.0 \text{ V}$) as a function of the number of monomer units. (G) STM topographic image ($V_s = -1.0 \text{ V}$, $V_s = 1.0 \text{ V}$) of short cGNRs resulting from annealing of a MAD-transferred sample of poly-1a to 420 °C for 10 min. (H) STM topographic image ($V_s = -2.0 \text{ V}$, $V_s = 1.0 \text{ V}$) of long cGNRs resulting from annealing of a MAD-transferred sample of poly-1b to 420 °C for 30 min.

units) and poly-**1b** (M = 7–12 kg mol⁻¹, 15–22 monomers units) (Figure 2G–H, SI Figure S4). Figure 2E,F shows histograms for cGNR length (as a function of monomer units) resulting from samples of poly-**1a** (N = 130) and poly-**1b** (N = 70). The mode, the mean, the median, the skewness (g), and even the kurtosis (κ) of the statistical length distribution of cGNRs mirrors the m/z distributions previously determined by MALDI-TOF MS of the original samples of poly-**1a** (Figure 2A) and poly-**1b** (Figure 2B). This remarkable correlation suggests that critical structural and functional parameters designed into a solution-synthesized GNR (co)polymer precursor, e.g., length, monomer sequence, and potentially even functional end groups, can be seamlessly translated into the structure of the resulting fully cyclized surface-supported GNRs.

To further illustrate the technological advancement enabled by MAD transfer we applied our technique to the synthesis of N₄-7-AGNR, a nanoribbon that, thus far, has been inaccessible using conventional bottom-up approaches. The structure of N₄-7-AGNRs (Scheme 2) can be derived from an alternating copolymer, poly-2, formed through a Suzuki-Miaura stepgrowth polymerization of anthracene-9,10-diyldiboronic (A) with 5,10-dibromopyrazino[2,3-g]quinoxaline (P). The alternating $(A-P)_n$ pattern of monomer building blocks in N_4 -7-AGNR is incompatible with the typical requirement for a symmetric repeat unit used in on-surface radical step-growth polymerizations of GNRs. At the same time, the oxidative cyclodehydrogenation of all peri-positions in poly-2 involves the formation of C-N bonds: a challenging transformation in solution yet readily accessible even at moderate temperatures on Au(111) surfaces. 16,23 The introduction of MAD transfer techniques enabled us to design a bottom-up synthesis of N₄-7-AGNR that takes advantage of the superior sequence control imparted by solution-based transition metal catalyzed cross-

Scheme 2. Bottom-Up Synthesis of N_4 -7-AGNR Segments using a MAD Transfer of *poly-2* Followed by Thermal Cyclodehydrogenation

coupling reactions, while retaining access to the surface-catalyzed cyclodehydrogenation sequence facilitated by the $\mathrm{Au}(111)$ substrate.

STM topographic images of short segments of $N_4\text{-}7\text{-}AGNR$ prepared by depositing a dispersion of 0.1 wt % poly-2 in a pyrene matrix onto a Au(111) substrate followed by annealing of the molecule decorated surface at 280 °C for 10 min are shown in Figure 3A. The uniform width (0.95 \pm 0.05 nm) and height (0.19 \pm 0.02 nm) of the molecular adsorbates is consistent with the expected dimensions of fully cyclo-

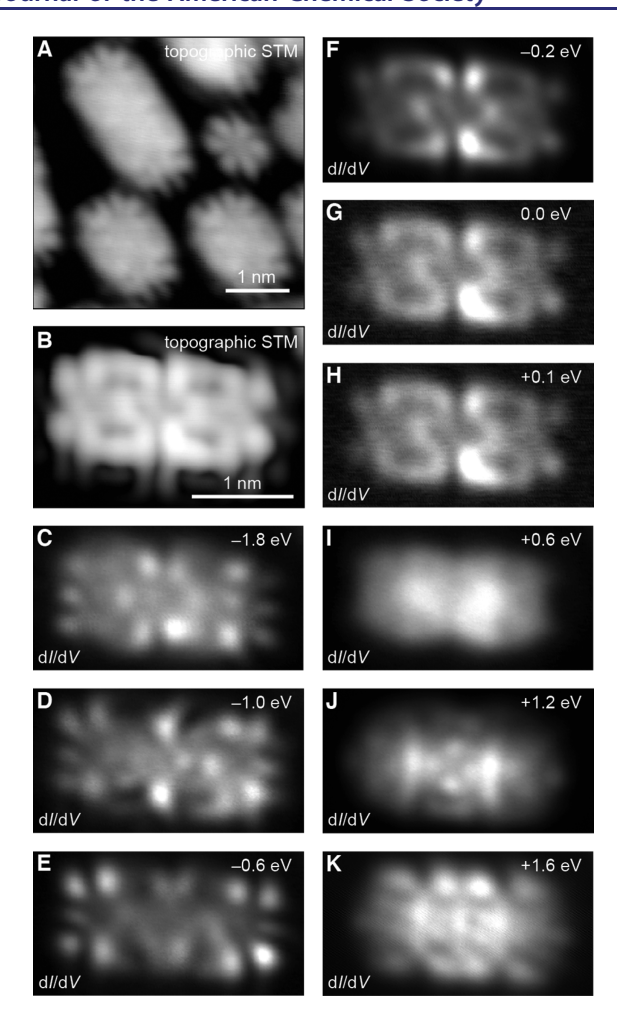


Figure 3. (A) STM topographic image ($V_s = -1.6$ V, $I_t = 50$ pA) of short segments of N₄-7-AGNR prepared by annealing a MAD transferred sample of *poly-2* to 280 °C for 10 min. (B) STM topographic image ($V_s = -0.05$ V, $I_t = 40$ pA) of a N₄-7-AGNR oligomer featuring an alternating pattern of anthracene and pyrazino[2,3-g]quinoxaline monomers. (C–K) dI/dV maps of the same oligomer at a biases ranging from -1.8 V to +1.6 V ((C–K) $f_V = 620$ Hz, $\Delta V_s = 10$ mV).

dehydrogenated N₄-7-AGNR segments. The longitudinal dimension is an integer multiple of 0.5 ± 0.05 nm commensurate with the average length added by either an anthracene or a pyrazino[2,3-g]quinoxaline unit. STM with passivated tips reveals that most N₄-7-AGNR feature an odd number of monomer units (>95%) and are terminated preferentially by anthracene groups. Figure 3B shows a topographic image of a N₄-7-AGNR oligomer featuring an alternating (A-P-A-P-A) pattern of three anthracene and two pyrazino[2,3-g]quinoxaline units. All eight pyrazino[2,3g quinoxaline nitrogen atoms have successfully undergone surface catalyzed cyclodehydrogenation. dI/dV maps of the same N₄-7-AGNR oligomer recorded across a bias of -1.8 V to +1.6 V (Figure 3C-K) show distinct features reflecting the molecular orbitals of the N₄-7AGNR, in full agreement with DFT calculations (SI Figure S7). The nonvanishing local density of states around the Fermi level ($E_{\rm F}$) (Figure 3F-H, SI Figure S7) is furthermore suggestive of p-type doping of N₄-7-AGNR on Au(111).

In summary, we report a hybrid bottom-up synthetic approach toward GNRs relying on a MAD transfer of

solution-synthesized polymer precursors onto a Au(111) substrate. Traceless removal of the bulk pyrene matrix followed by surface-assisted cyclodehydrogenation yields spatially isolated GNRs suitable for STM imaging and spectroscopy. We demonstrate that control over key structural parameters uniquely accessible through solution-based polymerization techniques can seamlessly be translated into the structure of the resulting surface-supported GNRs. The synergy between solution and surface-based bottom-up approaches enabled by our traceless MAD transfer technique provides synthetic avenues to complex functional GNR architectures that have thus far been inaccessible by conventional synthetic tools, but the possibility to transfer to any surface of choice (SI Figure S9) also paves the way for the integration of functional GNRs with lithographically patterned integrated circuit architectures.

ASSOCIATED CONTENT

Solution Supporting Information

The Supporting Information is available free of charge at https://pubs.acs.org/doi/10.1021/jacs.1c01355.

Synthetic procedures and characterization of poly-1 and poly-2 (PDF)

AUTHOR INFORMATION

Corresponding Author

Felix R. Fischer — Department of Chemistry, University of California, Berkeley, California 94720, United States; Materials Sciences Division, Lawrence Berkeley National Laboratory, Berkeley, California 94720, United States; Kavli Energy NanoSciences Institute at the University of California Berkeley and the Lawrence Berkeley National Laboratory, Berkeley, California 94720, United States; orcid.org/0000-0003-4723-3111; Email: ffischer@berkeley.edu

Authors

Ryan D. McCurdy — Department of Chemistry, University of California, Berkeley, California 94720, United States;
ocid.org/0000-0001-7319-4836

Peter H. Jacobse – Department of Physics, University of California, Berkeley, California 94720, United States Ilya Piskun – Department of Chemistry, University of California, Berkeley, California 94720, United States Gregory C. Veber – Department of Chemistry, University of

California, Berkeley, California 94720, United States

Daniel J. Rizzo — Department of Physics, University of
California, Berkeley, California 94720, United States;
orcid.org/0000-0003-4587-4863

Rafal Zuzak – Department of Physics, University of California, Berkeley, California 94720, United States; ⊚ orcid.org/ 0000-0001-6617-591X

Zafer Mutlu — Department of Electrical Engineering and Computer Sciences, University of California, Berkeley, California 94720, United States; orcid.org/0000-0002-2804-8618

Jeffrey Bokor – Department of Electrical Engineering and Computer Sciences, University of California, Berkeley, California 94720, United States; Materials Sciences Division, Lawrence Berkeley National Laboratory, Berkeley, California 94720, United States

Michael F. Crommie – Department of Physics, University of California, Berkeley, California 94720, United States; Materials Sciences Division, Lawrence Berkeley National Laboratory, Berkeley, California 94720, United States; Kavli Energy NanoSciences Institute at the University of California Berkeley and the Lawrence Berkeley National Laboratory, Berkeley, California 94720, United States; orcid.org/0000-0001-8246-3444

Complete contact information is available at: https://pubs.acs.org/10.1021/jacs.1c01355

Author Contributions

\$These authors contributed equally.

Notes

The authors declare no competing financial interest.

ACKNOWLEDGMENTS

This work was funded by the Office of Naval Research under N00014-19-1-2503 (synthesis of monomer and polymer precursors) and MURI Program N00014-16-1-2921 (STM imaging), by the U.S. Department of Energy, Office of Science, Office of Basic Energy Sciences, Materials Sciences and Engineering Division under Contract No. DE-AC02-05-CH11231 (Nanomachine program KC1203) (surface reaction, cyclization), by the National Science Foundation under Award No. CHE-1807474 (MAD transfer equipment development) and Award No. DMR-1839098 (SPM spectroscopy), and by the Center for Energy Efficient Electronics NSF Award 0939514 (data analysis). Portions of this work were carried out at the Molecular Foundry at Lawrence Berkeley National Laboratory (LBNL), supported by the Office of Science, Office of Basic Energy Sciences, of the U.S. Department of Energy (DOE) under contract no. DE-AC02-05CH11231, and at the Stanford Nano Shared Facilities (SNSF) at Stanford University, supported by the NSF under award ECCS-1542152. UC Berkeley NMR Facility usage was supported in part by NIH S10OD024998. P.H.J. acknowledges fellowship support from the Dutch Research Council through the Rubicon Award (019.182EN.18).

■ REFERENCES

- (1) Huang, H.; Wei, D.; Sun, J.; Wong, S. L.; Feng, Y. P.; Neto, A. H. C.; Wee, A. T. S. Spatially Resolved Electronic Structures of Atomically Precise Armchair Graphene Nanoribbons. *Sci. Rep.* **2012**, 2, 983.
- (2) Rizzo, D. J.; Veber, G.; Cao, T.; Bronner, C.; Chen, T.; Zhao, F.; Rodriguez, H.; Louie, S. G.; Crommie, M. F.; Fischer, F. R. Topological Band Engineering of Graphene Nanoribbons. *Nature* **2018**, *560*, 204–208.
- (3) Cai, J.; Ruffieux, P.; Jaafar, R.; Bieri, M.; Braun, T.; Blankenburg, S.; Muoth, M.; Seitsonen, A. P.; Saleh, M.; Feng, X.; Mullen, K.; Fasel, R. Atomically Precise Bottom-up Fabrication of Graphene Nanoribbons. *Nature* **2010**, *466*, 470.
- (4) Sun, Q.; Yao, X.; Gröning, O.; Eimre, K.; Pignedoli, C. A.; Müllen, K.; Narita, A.; Fasel, R.; Ruffieux, P. Coupled Spin States in Armchair Graphene Nanoribbons with Asymmetric Zigzag Edge Extensions. *Nano Lett.* **2020**, *20*, 6429–6436.
- (5) Ruffieux, P.; Wang, S.; Yang, B.; Sanchez-Sanchez, C.; Liu, J.; Dienel, T.; Talirz, L.; Shinde, P.; Pignedoli, C. A.; Passerone, D.; Dumslaff, T.; Feng, X.; Mullen, K.; Fasel, R. On-Surface Synthesis of Graphene Nanoribbons with Zigzag Edge Topology. *Nature* **2016**, 531, 489–492.
- (6) Gröning, O.; Wang, S.; Yao, X.; Pignedoli, C. A.; Borin Barin, G.; Daniels, C.; Cupo, A.; Meunier, V.; Feng, X.; Narita, A.; Mullen, K.; Ruffieux, P.; Fasel, R. Engineering of Robust Topological Quantum Phases in Graphene Nanoribbons. *Nature* **2018**, *560*, 209–213.

- (7) Rizzo, D. J.; Veber, G.; Jiang, J.; McCurdy, R.; Cao, T.; Bronner, C.; Chen, T.; Louie, S. G.; Fischer, F. R.; Crommie, M. F. Inducing Metallicity in Graphene Nanoribbons via Zero-Mode Superlattices. *Science* **2020**, *369*, 1597LP–1603.
- (8) Yoon, K. Y.; Dong, G. Liquid-Phase Bottom-up Synthesis of Graphene Nanoribbons. *Mater. Chem. Front.* **2020**, *4*, 29–45.
- (9) Talirz, L.; Ruffieux, P.; Fasel, R. On-Surface Synthesis of Atomically Precise Graphene Nanoribbons. *Adv. Mater.* **2016**, 28, 6222–6231.
- (10) Chen, Z.; Narita, A.; Müllen, K. Graphene Nanoribbons: On-Surface Synthesis and Integration into Electronic Devices. *Adv. Mater.* **2020**, 32, 1–26.
- (11) Von Kugelgen, S.; Piskun, I.; Griffin, J. H.; Eckdahl, C. T.; Jarenwattananon, N. N.; Fischer, F. R. Templated Synthesis of End-Functionalized Graphene Nanoribbons through Living Ring-Opening Alkyne Metathesis Polymerization. *J. Am. Chem. Soc.* **2019**, *141*, 11050–11058.
- (12) Mateo, L. M.; Sun, Q.; Liu, S. X.; Bergkamp, J. J.; Eimre, K.; Pignedoli, C. A.; Ruffieux, P.; Decurtins, S.; Bottari, G.; Fasel, R.; Torres, R. On-Surface Synthesis and Characterization of Triply Fused Porphyrin-Graphene Nanoribbon Hybrids. *Angew. Chem., Int. Ed.* **2020**, *59*, 1334–1339.
- (13) Urgel, J. I.; Di Giovannantonio, M.; Gandus, G.; Chen, Q.; Liu, X.; Hayashi, H.; Ruffieux, P.; Decurtins, S.; Narita, A.; Passerone, D.; Yamada, H.; Liu, S.; Mullen, K.; Pignedoli, C.; Fasel, R. Overcoming Steric Hindrance in Aryl-Aryl Homocoupling via On-Surface Copolymerization. *ChemPhysChem* **2019**, *20*, 2360–2366.
- (14) Radocea, A.; Sun, T.; Vo, T. H.; Sinitskii, A.; Aluru, N. R.; Lyding, J. W. Solution-Synthesized Chevron Graphene Nanoribbons Exfoliated onto H: Si(100). *Nano Lett.* **2017**, *17*, 170–178.
- (15) Shekhirev, M.; Vo, T. H.; Kunkel, D. A.; Lipatov, A.; Enders, A.; Sinitskii, A. Aggregation of Atomically Precise Graphene Nanoribbons. *RSC Adv.* **2017**, *7*, 54491–54499.
- (16) Piskun, I.; Blackwell, R.; Jornet-Somoza, J.; Zhao, F.; Rubio, A.; Louie, S. G.; Fischer, F. R. Covalent C-N Bond Formation through a Surface Catalyzed Thermal Cyclodehydrogenation. *J. Am. Chem. Soc.* **2020**, *142*, 3696–3700.
- (17) Jacobse, P. H.; McCurdy, R. D.; Jiang, J.; Rizzo, D. J.; Veber, G.; Butler, P.; Zuzak, R.; Louie, S. G.; Fischer, F. R.; Crommie, M. F. Bottom-up Assembly of Nanoporous Graphene with Emergent Electronic States. *J. Am. Chem. Soc.* **2020**, *142*, 13507–13514.
- (18) Vo, T. H.; Shekhirev, M.; Kunkel, D. A.; Morton, M. D.; Berglund, E.; Kong, L.; Wilson, P. M.; Dowben, P. A.; Enders, A.; Sinitskii, A. Large-Scale Solution Synthesis of Narrow Graphene Nanoribbons. *Nat. Commun.* **2014**, *5*, 1–8.
- (19) Goldfarb, J. L.; Suuberg, E. M. Vapor Pressures and Enthalpies of Sublimation of Ten Polycyclic Aromatic Hydrocarbons Determined via the Knudsen Effusion Method. *J. Chem. Eng. Data* **2008**, *53*, 670–676.
- (20) Judy, C. L.; Pontlkos, N. M.; Acree, W. E. Solubility of Pyrene in Binary Solvent Mixtures Containing Cyclohexane. *J. Chem. Eng. Data* **1987**, 32, 60–62.
- (21) Roux, M. V.; Temprado, M.; Chickos, J. S.; Nagano, Y. Critically Evaluated Thermochemical Properties of Polycyclic Aromatic Hydrocarbons. *J. Phys. Chem. Ref. Data* **2008**, 37, 1855—1996.
- (22) Schleicher, S.; Borca, B.; Rawson, J.; Matthes, F.; Bürgler, D. E.; Kögerler, P.; Schneider, C. M. Ultra-High Vacuum Deposition of Pyrene Molecules on Metal Surfaces. *Phys. Status Solidi Basic Res.* **2018**, 255, 1–7.
- (23) Li, Y. L.; Zee, C. Te; Lin, J. B.; Basile, V. M.; Muni, M.; Flores, M. D.; Munárriz, J.; Kaner, R. B.; Alexandrova, A. N.; Houk, K. N.; Tolbert, S. H.; Rubin, Y. Fjord-Edge Graphene Nanoribbons with Site-Specific Nitrogen Substitution. *J. Am. Chem. Soc.* **2020**, *142*, 18093—18102.